Acta Pharmacologica Sinica

www.nature.com/aps

ARTICLE

Melatonin ameliorates bleomycin-induced pulmonary fibrosis via activating NRF2 and inhibiting galectin-3 expression

Yue-jiao Lan[1,2], Ming-han Cheng[1], Hui-min Ji[3], Yu-qian Bi[3], Yong-yue Han[1], Chong-yang Yang[3], Xuan Gu[4], Jian Gao[1] and Hong-liang Dong[1]

Pulmonary fibrosis (PF) is a chronic interstitial lung disease with no effective therapies. Galectin-3 (Gal-3), a marker of oxidative stress, plays a key role in the pathogenesis of PF. Fibroblast-myofibroblast differentiation (FMD) is an important source of fibrotic cells in PF. Previous studies showed that melatonin (MT) exerted anti-fibrotic effect in many diseases including PF through its antioxidant activity. In the present study we investigated the relationships among Gal-3, NRF2, ROS in FMD and their regulation by MT. We established an in vitro model of FMD in TGF-β1-treated human fetal lung fibroblast1 (HFL1) cells and a PF mouse model *via* bleomycin (BLM) intratracheal instillation. We found that Gal-3 expression was significantly increased both in vitro and in vivo. Knockdown of Gal-3 in HFL1 cells markedly attenuated TGF-β1-induced FMD process and ROS accumulation. In TGF-β1-treated HFL1 cells, pretreatment with NRF2-specific inhibitor ML385 (5 μM) significantly increased the levels of Gal-3, α-SMA and ROS, suggesting that the expression of Gal-3 was regulated by NRF2. Treatment with NRF2-activator MT (250 μM) blocked α-SMA and ROS accumulation accompanied by reduced Gal-3 expression. In BLM-induced PF model, administration of MT (5 $mg \cdot kg^{-1} \cdot d^{-1}$, ip for 14 or 28 days) significantly attenuated the progression of lung fibrosis through up-regulating NRF2 and down-regulating Gal-3 expression in lung tissues. These results suggest that Gal-3 regulates TGF-β1-induced pro-fibrogenic responses and ROS production in FMD, and MT activates NRF2 to block FMD process by down-regulating Gal-3 expression. This study provides a useful clue for a clinical strategy to prevent PF.

Keywords: pulmonary fibrosis; fibroblast-myofibroblast differentiation; galectin-3; NRF2; ROS; melatonin

Acta Pharmacologica Sinica (2023) 44:1029–1037; https://doi.org/10.1038/s41401-022-01018-x

INTRODUCTION

The formation of pulmonary scarring induced by autoimmune diseases, environmental and occupational exposures, pneumonia, and side effects of certain drugs is known as pulmonary fibrosis (PF), and its irreversible pathogenesis and severe impairment of lung function make it one of the most lethal respiratory diseases [1]. PF with unknown etiology is termed idiopathic pulmonary fibrosis (IPF), whose median survival time from diagnosis is 3~4 years and the incidence continues to rise [2]. Currently, lung transplantation is the only intervention shown to extend the life expectation of patients with IPF [3]. Notably, one of the major complications with infection of the novel coronavirus severe acute respiratory syndrome coronavirus-2 (SARS-CoV-2) is PF, which leads to increased chronic dyspnea and impaired quality of life in patients with COVID-19 [4]. Viral-induced acute respiratory distress syndrome (ARDS) and PF share many risk factors and biological processes, including gender, aging, hypertension and diabetes [5], and lung epithelial cells and fibroblasts also participated in COVID-19 induced PF [6]. Therefore, investigating the pathogenesis of PF and searching for new therapeutic targets is a novel strategy to treat severe COVID-19 and prevent the possible long-term fibrotic consequences after current pandemic.

Accumulating evidences suggest that the pathological myofibroblast cells in PF mainly originate from epithelial cells and fibroblasts, and these processes are termed as EMT (epithelial-mesenchymal transition) and FMD (fibroblast-myofibroblast differentiation) respectively. Galectin-3 (Gal-3), the only chimera-type of the β-galactoside-binding lectin family, has been found to play pivotal role in TGF-β1 induced EMT in lung fibrosis and Gal-3 inhibitor TD139 has been proved to be effective in lung fibrosis model and IPF patients [7, 8]. However, engagement of Gal-3 in FMD process and the related mechanism remain poorly understood.

As a marker of oxidative stress, Gal-3 has been shown to be potentially associated with perturbations in mitochondrial homeostasis and the subsequent formation of reactive oxygen species (ROS) and glutathione (GSH) depletion [9–12]. Recombinant Gal-3 could stimulate ROS production in neutrophils [13] and monocytes [14] in a dose-dependent manner and increased Gal-3 contributed to superoxide production [15]. NRF2 is known as the major negative regulator of ROS and oxidative stress [16]. Our previous studies demonstrated that NRF2 attenuated the EMT process in PF through inhibition of the Numb or high-mobility group box 1 (HMGB1) pathway [17, 18]. Melatonin (MT, N-acetyl-5-methoxytryptamine), a hormone mainly secreted by the pineal

[1]Pediatric Translational Medicine Institute, Shanghai Children's Medical Center, School of Medicine, Shanghai Jiao Tong University, Shanghai 200120, China; [2]Jilin Province People's Hospital, Changchun 130021, China; [3]Dalian Medical University, Dalian 116023, China and [4]3201 Hospital, Hanzhong 723000, China
Correspondence: Jian Gao (gaojianayfy@163.com) or Hong-liang Dong (hldongscmc@163.com)
These authors contributed equally: Yue-jiao Lan, Ming-han Cheng

Received: 1 July 2022 Revised: 19 October 2022 Accepted: 19 October 2022
Published online: 4 November 2022

gland, was found to activate NRF2 and inhibit the EMT process, so exerted anti-fibrogenic activity in many diseases including PF [19, 20]. Whether NRF2 plays a role in FMD process and its relationship with Gal-3 in excessive ROS production in pulmonary fibrosis remain to be elucidated.

In this study, we established an in vitro FMD model by employing TGF-β1 treated HFL1 cells and an in vivo PF model using tracheal drip in C57BL/6 J mice with BLM. With these models we revealed that Gal-3 regulated TGF-β1-induced pro-fibrogenic responses in FMD, and MT-mediated NRF2 activation could down-regulate Gal-3, attenuate ROS production and improve FMD in PF. These findings uncovered a NRF2-Gal-3-ROS-FMD axis mediating the protective effect of MT on pulmonary fibrosis, providing a useful clue for a clinical strategy against the disease.

MATERIALS AND METHODS

Experimental animals

Male C57BL/6 J mice, 8–10 weeks old, were purchased from Institute of Genome Engineered Animal Models for Human disease of Dalian Medical University. Mice were housed under Specific Pathogen Free (SPF) conditions at controlled temperature (25 ± 2 °C), maintained in a 12-h light-dark cycle, and with free access to water and normal diet. All animal experiments were approved by the Dalian Medical University Animal Protection and Use Committee (Ethical approval number: AEE19013).

BLM-induced PF model

PF animal model was established by intratracheal injection of 4.5 mg/kg BLM (Anhui Pharmaceutical Co, Anhui, China) as described previously, and the control group was injected with equal volume of normal saline [21, 22]. For drug treatment, MT (5 mg·kg^{-1}·d^{-1}) was administered every day by intraperitoneal injection (ip). A total of 80 male mice were randomly divided into four groups, with 20 mice per group, designated as the saline group, BLM + saline group, BLM + MT group and saline + MT group. On day 14 and day 28, lung tissues were collected and fixed for the following assays.

Histopathological assessment

Lungs of mice were removed from euthanized mice for H&E staining and immunohistochemical analysis. Samples from each group were embedded in paraffin and made into 5 μm slices. The slices were stained with Hematoxylin-Eosin (H&E, C0105s, Beyotime Biotechnology, Shanghai, China) and Masson trichrome (D026, Nanjing Jiancheng Bioengineering Institute, Nanjing, China) to assess histopathological changes in the lungs. In H&E staining, the Digital Fibrosis Scale (Ashcroft score) was used to assess the severity of fibrosis. After observing fifteen areas of lung tissue for day 28 with ×100 magnification, they were evaluated with a score of 0 (normal) to 8 (complete fibrosis) [23].

Immunohistochemistry assay

Tissue sections were permeabilized with 0.3% Triton X-100 for 10 min, blocked with antigen repair and goat serum for 15 min and then incubated with Gal-3 (ab76245, Abcam, Cambridge, UK) and Col-I (bs-10423 R, Bioss, Massachusetts, USA) specific antibodies separately. Images were captured using the optical microscope (Leica DM2000, Germany). The number of positively stained cells in the lung tissue was quantified using Image J.

Immunofluorescence staining

Cells were fixed in 4 % paraformaldehyde for 10 min and permeabilized with 0.1 % Triton X-100 for 10 min. For the IF staining of lung tissues, paraffin sections were firstly subjected to deparaffinization and rehydration followed by retrieving antigens. Thereafter, cells or sections were incubated with 5% bovine serum albumin for 30 min and primary antibodies overnight at 4 °C. Cells or sections were incubated with goat anti-rabbit IgG (1:100 dilution) or goat anti-mouse IgG (1:100 dilution) for 1 h at room temperature. After washing with PBS, cells or sections were stained with 4′,6-Diamino-2-phenylindole (DAPI, 1:100 dilution). Images were taken on an inverted fluorescence microscope (DMI3000B, Leica, Germany).

Cell counting kit-8 (CCK8) assay

HFL1 cells were purchased from the Chinese Academy of Sciences Cell Bank (Shanghai, China). HFL1 cells were seeded to 96-well plate at a density of 5×10^3 cells per well. The cells were then treated with 0.1% DMSO as vehicle control and MT with various concentrations (0–500 μM) for 24 h. The medium was replaced with a 100 μL fresh medium containing a 10 μL CCK8 reagent (MA0218, Meilunbio, Dalian, China). After incubation at 37 °C for 4 h, The *OD* absorbance readings were recorded at 450 nm with SpectraMax 190a (Molecular Devices, US). The cell viability was calculated using the following formula: Cell viability (%) = $(OD_{\text{treatment}} - OD_{\text{blank}})/(OD_{\text{control}} - OD_{\text{blank}}) \times 100$.

Cell culture

The cells were cultured in Ham's F-12 K (PM150910, Procell, Wuhan, China) supplemented with 10% fetal bovine serum (FBS, 10099141 C, Gibco, USA) and 1% streptomycin-penicillin (ABT920, G-CLONE, Beijing, China). All cell cultures were maintained at 37 °C with 5% CO_2.

Western blot analysis

Frozen lung tissues and pulmonary fibroblasts were harvested in RIPA Digest Buffer. The supernatant was collected, and protein concentration was measured using the BCA Protein Assay Reagent Kit. Equal amounts of protein were electrophoretically separated in SDS-polyacrylamide gels and then transferred onto polyvinylidene difluoride membranes (PVDF, IPVH00010, Millipore, USA). The blot was blocked with 5% skim milk for 1 h at room temperature and probed overnight at 4 °C by incubation with the primary antibodies, including anti-NRF2 (ab31163, Abcam, Cambridge, UK), anti-Gal-3 (ab76245, Abcam, Cambridge, UK), anti-α-SMA (ab5694, Abcam, Cambridge, UK), or anti-GAPDH (2118, CST, Boston, USA) antibodies. After being washed with Tris Buffered Saline with Tween (TBST), the membranes were subsequently incubated with secondary horseradish peroxidase conjugated anti-rabbit antibodies at 25 °C for 2 h. Finally, membranes were analyzed by Oddessy Clx.

Gal-3 small interference RNA (siRNA)

A mixture of Gal-3 small interference RNA (siRNA) and Lipofectamine 2000 was added to HFL1 cells with a growth confluence of 60%–70%, according to the manufacturer's instructions. Gal-3 siRNA and scramble siRNA were purchased from Gene Pharma (Shanghai, China). The Gal-3 primer sequence was orthogonal to 5′-GCCCAAUGCAAACAGAAUUTT-3′ and the reverse is 5′-AAUUCU GUUUGCAUUGGGCTT-3′.

Assessment of oxidative stress

Intracellular oxidative stress was determined using dihydroethidium (DHE, S0063, Beyotime Biotechnology, Shanghai, China) and DCFH-DA active oxygen ROS fluorescent probe (S0033, Beyotime Biotechnology, Shanghai, China) according to the manufacturer's instructions. Briefly, the cells were incubated with 5 μM of DHE at 37 °C for 30 min, or 10 μM of DCFH-DA at 37 °C for 20 min, then the ROS images were observed by SpectraMax 190a (Molecular Devices, California, USA) at ×20 magnification.

Biochemical assay

Lung tissue homogenate was taken for glutathione (GSH), malondialdehyde (MDA), total superoxide dismutase (T-SOD)

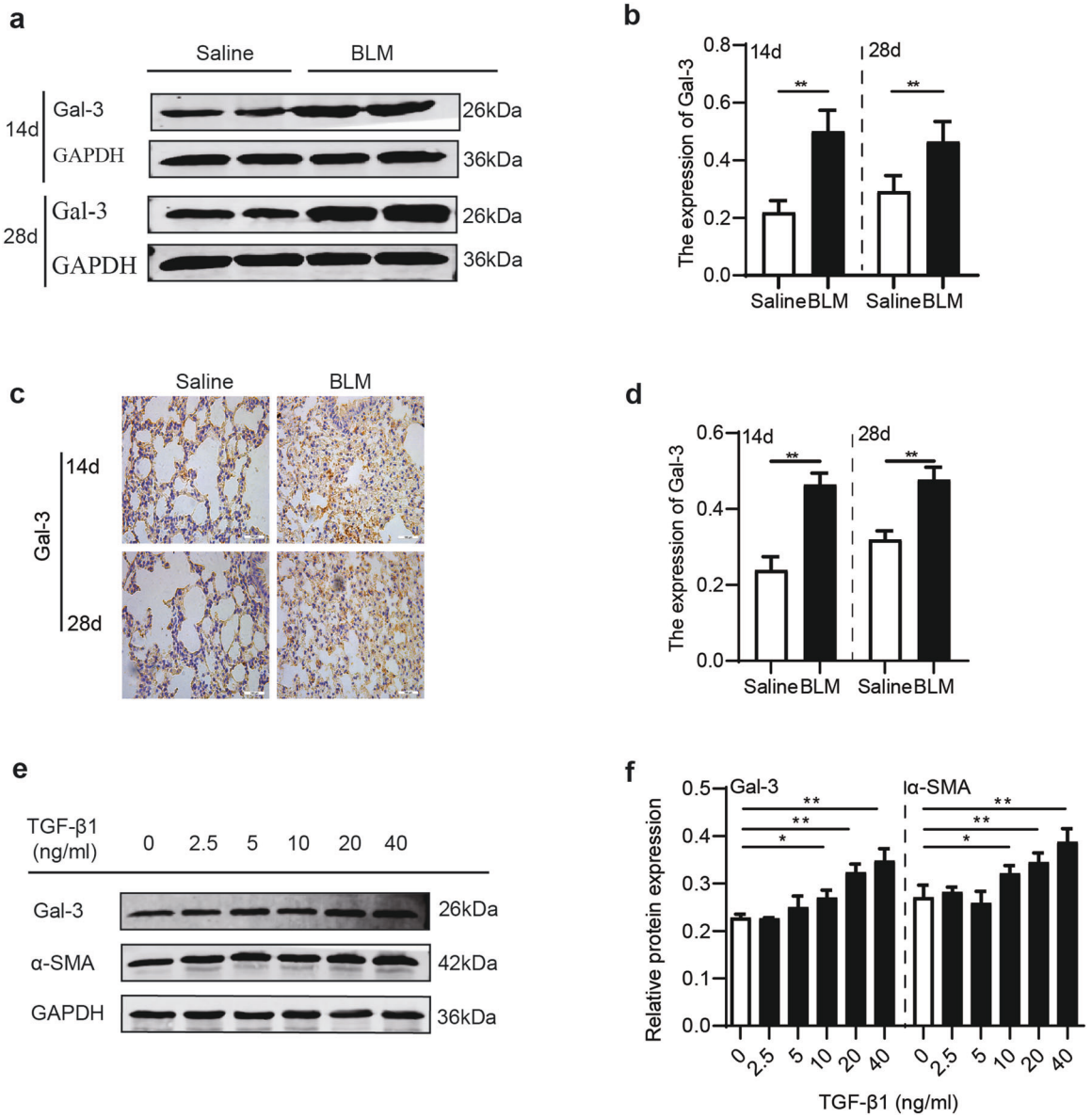

Fig. 1 Increased Gal-3 expression in BLM induced PF mice and FMD process in HFL1 cells. PF was induced by intratracheal instillation of BLM in vivo. FMD model was constructed by further stimulation of HFL1 with TGF-β1 in vitro. Western blot results (**a**) and statistical analysis (**b**) of Gal-3 in BLM-induced fibrotic lungs. Relative protein levels were normalized to GAPDH ($n = 3$), $^{**}P < 0.01$ versus the Saline group. Immunohistochemistry results (**c**) and statistical analysis (**d**) of Gal-3 in the BLM-induced fibrotic lungs ($n = 3$). Scale bar: 100 μm. $^{**}P < 0.01$ versus the Saline group. Western blot results (**e**) and quantitation (**f**) of Gal-3 with α-SMA protein in FMD process of TGF-β1 stimulated HFL1 cells. Relative protein levels were normalized to GAPDH ($n = 3$), $^{*}P < 0.01$, $^{**}P < 0.01$ versus the Control group.

and glutathione peroxidase (GSH-Px) assay according to the manufacturer's protocols of GSH, MDA, T-SOD and GSH-Px assay kit (Nanjing Jiancheng Bioengineering Institute, Nanjing, China).

Statistical analysis

Data are expressed as mean ± standard deviation (SD). Statistical analysis was performed using IBM SPSS Statistics 25 (SPSS software, International Business Machines Corporation, New York, USA), and bar graphs were plotted using GraphPad Prism 8 (GraphPad Software, San Diego, CA, USA). For differences between two groups, independent samples *t*-tests were used. Comparisons between groups were analyzed using one-way analysis of variance (ANOVA) followed by Tukey *post hoc* test. *P*-values < 0.05 were considered statistically significant.

RESULTS

Gal-3 expression is up-regulated in fibrotic lungs of BLM challenged mice and in in vitro FMD model

Gal-3 expression could be induced in activated macrophages and fibroblasts under the conditions of tissue injury and stress such as infection and irradiation [24, 25]. Gal-3 contributes to fibroblasts activation in different tissues including kidney, liver and heart, and is involved in EMT process, scar formation and tissue structure destruction under pathological conditions [26]. To explore the roles of Gal-3 in PF, we firstly examined the expression level of Gal-3 in lung tissues of BLM-induced PF mice. The results showed that Gal-3 was increased significantly after BLM administration compared with the saline group (Fig. 1a–d). In an in vitro FMD model, TGF-β1 up-regulated Gal-3 level in HFL1 cells in a dose-dependent manner, accompanied by expression of α-SMA (Fig. 1e,

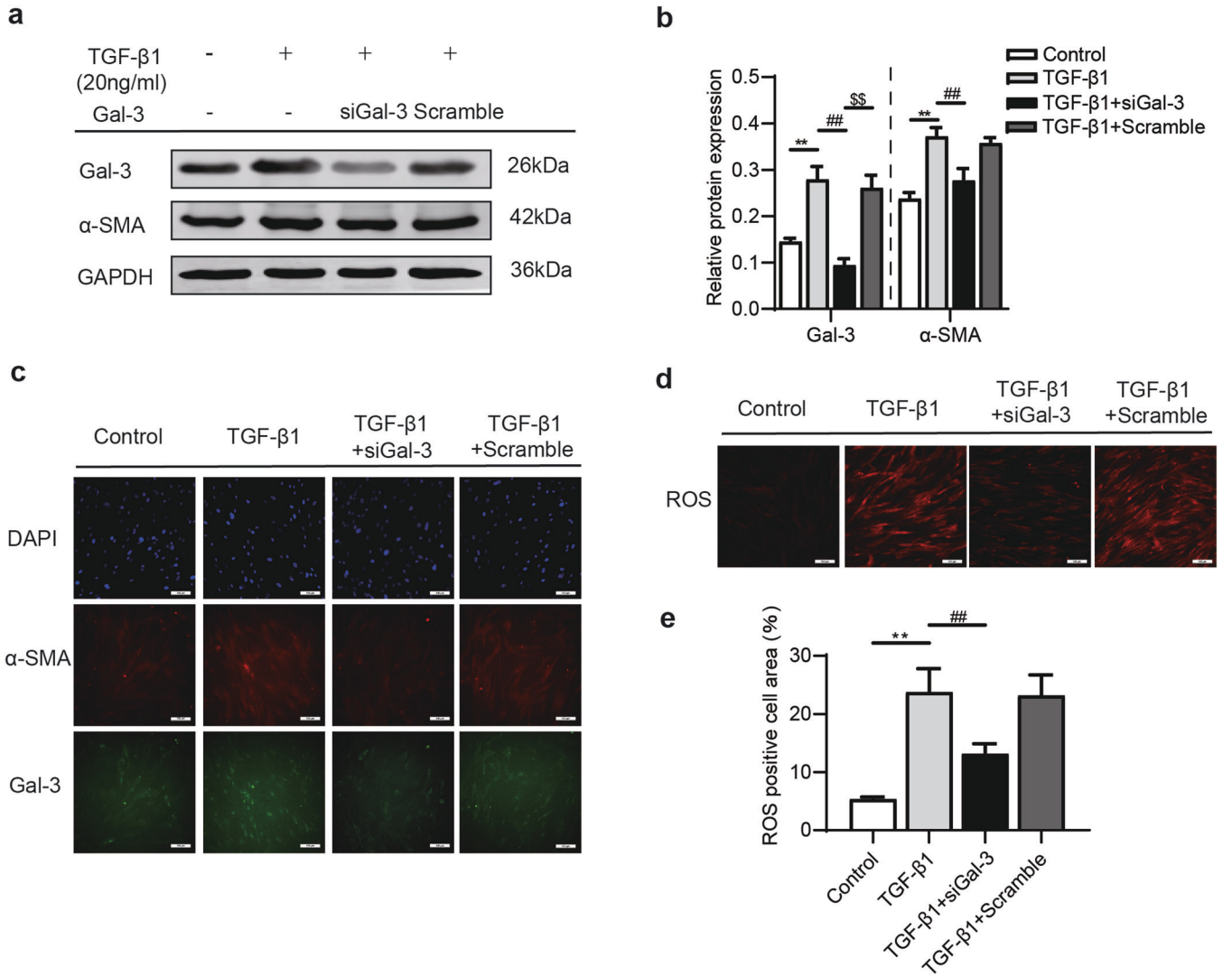

Fig. 2 Knockdown of Gal-3 attenuated TGF-β1-induced FMD process and the degree of ROS accumulation. HFL1 cells were transfected by Gal-3 siRNA or negative siRNA, and then stimulated with TGF-β1(20 ng/mL) for 24 h. Western blot results (**a**) and statistical analysis (**b**) of Gal-3 and α-SMA level. Relative protein levels were normalized to GAPDH ($n = 3$). Representative immunofluorescence staining of α-SMA (red) and Gal-3 (green) in HFL1. Scale bar: 100 μm (**c**). Dihydroethidium (DHE) stain was performed to measure ROS level (**d**). ROS-positive area was quantified using Image J software ($n = 3$) (**e**). $^{**}P < 0.01$ versus the Control group, $^{\#\#}P < 0.01$ versus the TGF-β1 group, $^{\$\$}P < 0.01$ versus the TGF-β1 + siGal-3 group.

f), a hallmark of FMD process. These data indicated that Gal-3 expression was positively correlated with FMD in PF.

Gal-3 knockdown attenuated FMD and accumulation of ROS in in vitro FMD model

In order to further elucidate the roles of Gal-3 in FMD, we knocked down Gal-3 expression in TGF-β1 induced FMD model in HFL1 cells using small interfering RNA. Considering that FMD often occurs with dysregulation of oxidative stress characterized by excessive accumulation of ROS [27, 28], which contributes to production and remodeling of ECM [29], we also assessed ROS accumulation in FMD after Gal-3 knockdown. The results showed that knocking down the expression of Gal-3 reduced the TGF-β1 induced α-SMA (Fig. 2a, b, c) and ROS (Fig. 2d, e) production in HFL1 cells. Collectively, these results pointed out that Gal-3 is actively engaged in TGF-β1 induced α-SMA and ROS accumulation in FMD.

NRF2 inhibition up-regulated Gal-3, α-SMA level and ROS accumulation in in vitro FMD model

The lung is a key site of gas exchange, so the airways are often exposed to a highly oxidative microenvironment, leading to disruption of redox homeostasis [30, 31]. Consistently, PF is also characterized by imbalance between ROS production and anti-oxidant capacity. NRF2 is known as a master regulator of the antioxidant response that drives adaptive cellular defense against oxidative stress and plays a protective role in PF. Based upon our finding that Gal-3, a marker of oxidative stress, mediated TGF-β1 induced α-SMA and ROS accumulation in FMD, we further try to clarify the regulatory effect of NRF2 on Gal-3 in the process of FMD. ML385, a NRF2-specific inhibitor [32], increased Gal-3, α-SMA (Fig. 3a, b) and ROS level in TGF-β1-induced HFL1 cells (Fig. 3c, d), indicating that the expression of Gal-3 was regulated by NRF2 in FMD.

MT-mediated NRF2 activation down-regulated Gal-3 and suppressed TGF-β1 induced FMD in vitro

MT is a potential activator of NRF2 [33] mediating strong antioxidant activity by up-regulating the expression and activity of endogenous antioxidants, and removing ROS by radical scavenging [34–36]. Herein, we explored whether MT could regulate NRF2 and Gal-3 to suppress oxidative stress in FMD. The cell counting kit-8 (CCK8) assay in HFL1 cells showed that MT

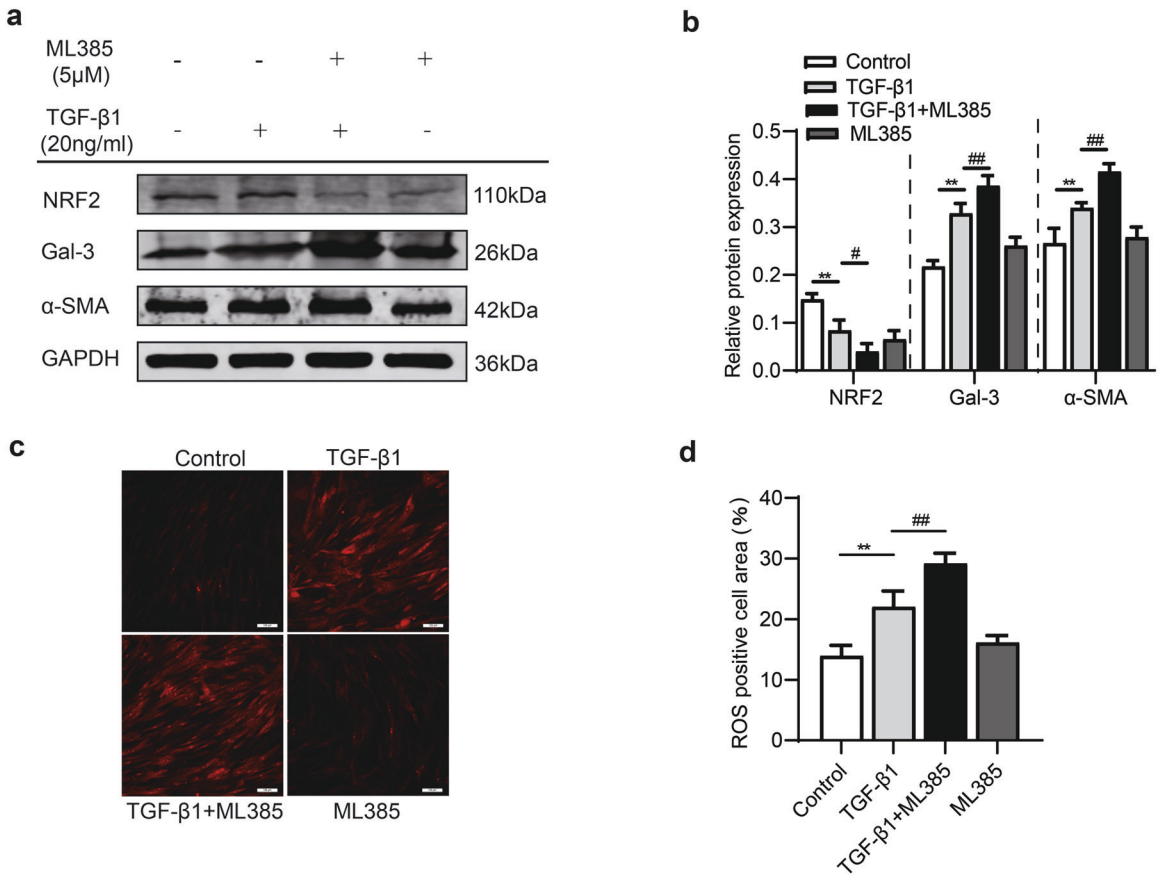

Fig. 3 Application of ML385 upregulated α-SMA, Gal-3 and ROS production. ML385 (5 μM) was preincubated with HFL1 cells for 24 h, after which TGF-β1 (20 ng/mL) and culture medium were added for 24 h treatment. Western blot bands (**a**) and quantitation (**b**) of NRF2, Gal-3, and α-SMA levels after ML385 administration. Relative protein levels were normalized to GAPDH ($n = 3$). **c**, **d** Dihydroethidium (DHE) detection of ROS accumulation ($n = 3$). $^{**}P < 0.01$ versus the Control group, $^{\#}P < 0.05$, $^{\#\#}P < 0.01$ versus the TGF-β1 group.

did not have cytotoxicity at concentrations up to 500 μM (Fig. 4a), and the Western-blot results suggested that MT increased NRF2 expression in a dose-dependent manner (Fig. 4b, c). IF staining further revealed that MT induced nuclear accumulation of NRF2 in HFL1 cells (Fig. 4d). Besides activation of NRF2, MT also inhibited the expression level of Gal-3, α-SMA as well as ROS accumulation in TGF-β1 stimulated HFL1 cells (Fig. 4e, f, g, h). All these results suggested that MT could significantly activate NRF2 and down-regulate Gal-3 in HFL1 cells to inhibit FMD and ROS production.

MT ameliorates BLM-induced PF by reducing oxidative stress level in vivo

Next, we asked if MT could exhibit anti-fibrosis effect by regulating oxidative stress level in vivo. MT treatment significantly reduced the degree of fibrosis and oxidative stress in lung tissues of BLM-induced PF mice (Fig. 5). As shown in Fig. 5b, c, MT significantly ameliorated BLM induced severe disruption of alveolar structure, thicker alveolar septa, infiltration of inflammatory cells (Fig. 5b) and higher Ashcroft score (Fig. 5c). Masson staining and immunohistochemistry staining of Col-I results showed that MT rescued BLM-induced collapse of alveolar spaces, pulmonary interstitial collagen deposition (Fig. 5d) and Col-I expression (Fig. 5e, f). Besides above histologic analysis on fibrosis, we also tested some important biomarkers of oxidative stress including GSH, MDA, T-SOD and GSH-Px. Compared with control mice, BLM treated mice showed increased MDA, and decreased T-SOD, GSH, and GSH-Px, which had all been corrected by MT treatment (Fig. 5g~j). Thus, these findings suggest that MT could ameliorate BLM-induced oxidative stress and PF in vivo.

MT induced NRF2 up-regulation and Gal-3 down-regulation in lung tissues of BLM-induced PF in vivo

Since MT was shown to regulate NRF2 and Gal-3 in HFL1 cells in vitro, we further explored whether MT exerts its anti-fibrotic effect through activating NRF2 as well as suppressing Gal-3 levels in vivo. As shown in Fig. 6, MT treatment reversed BLM induced NRF2 decrease and Gal-3, α-SMA increase in lung tissues (Fig. 6a–d). IF staining also showed similar effect of MT on Gal-3 and α-SMA levels (Fig. 6e, f). In summary, our data demonstrated that MT alleviates PF by inhibiting Gal-3 expression in vivo.

DISCUSSION

Gal-3 is of importance for the symptoms and progression of various fibrosis diseases including liver fibrosis [37], renal fibrosis [38] and PF [7], with Gal-3 inhibitors like TD139 showing anti-fibrotic efficacy in preclinical PF model and phase 1/2 clinical trial in IPF patients [7, 8, 39]. Mechanisms uncovered for Gal-3 mainly focused on its modulation of EMT process, either by activating the AKT/GSK3β/β-catenin signaling pathway [40] or by galectin-3-glycan interactions [41]. In this study, we found that Gal-3 was also engaged in FMD and oxidative stress response in PF. Knockdown of Gal-3 expression could attenuate FMD and ROS accumulation in the in vitro model. Gal-3 expression was regulated by the classical antioxidant protein NRF2, and in BLM induced PF model MT administration up-regulated NRF2, down-regulated Gal-3 and effectively attenuated extracellular matrix (ECM), collagen deposition and ROS production at the onset of PF. We therefore propose that Gal-3 could be considered as a key pro-oxidative stress

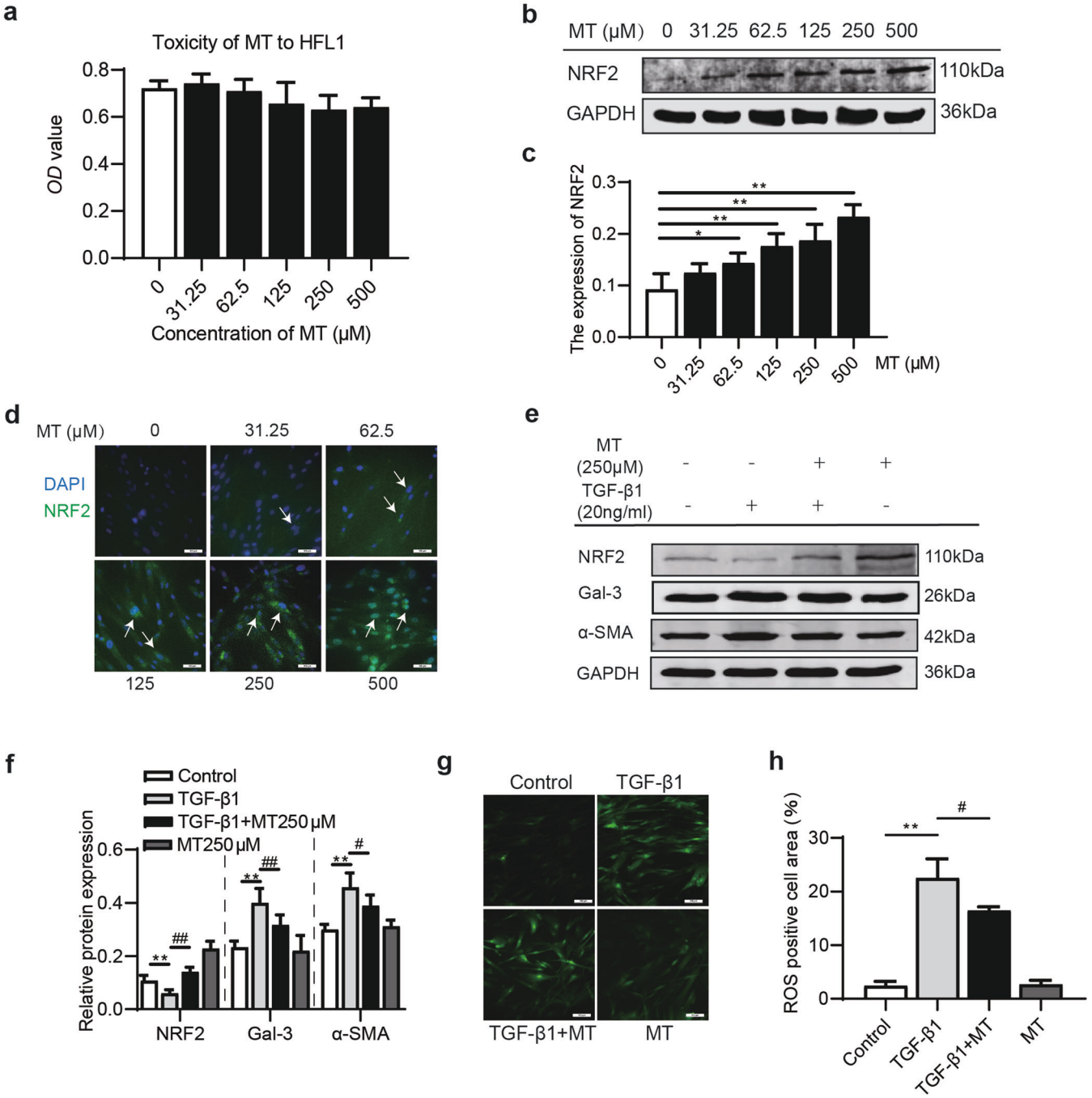

Fig. 4 Regulation by MT in NRF2 activation, Gal-3 expression and ROS accumulation in TGF-β1-treated HFL1 cells. a HFL1 cells were treated with different concentrations of MT (0–500 μM) for 24 h. The effect of MT at gradient concentrations on cell viability was assayed with CCK8 kit. Western blot (**b**) and statistical analysis (**c**) for the change of NRF2 expression level, relative protein levels were normalized to GAPDH ($n = 3$), $^{*}P < 0.05$, $^{**}P < 0.01$ versus 0 group. **d** Immunofluorescence was used to observe NRF2 subcellular expression (the typical nuclear accumulation of NRF2 is indicated by white arrows). Scale bars: 100 μm. Western blot (**e**) and quantitation (**f**) of NRF2, Gal-3 and α-SMA level in TGF-β1-stimulated HFL1 cells. Relative protein levels were normalized to GAPDH ($n = 3$), $^{**}P < 0.01$ versus the Control group, $^{\#}P < 0.05$, $^{\#\#}P < 0.01$ versus the TGF-β1 group. **g**, **h** ROS stain kit was used to measure ROS level.

mediator during TGF-β1 induced FMD process, thereby contributing to the pathogenesis of PF.

Although we demonstrated here that Gal-3 participated in ROS production in FMD, the underlying mechanism remains to be clarified. It is known that NADPH oxidase (NOX) is an important source of ROS production [42, 43]. He J et al reported that Gal-3 was involved in the production of ROS in cardiac fibroblasts by inducing NOX expression, especially NOX4 [44]. Similarly, Gal-3 stimulated the expression of NOX4 in cardiac myocytes and regulated the level of NOX4-derived ROS during myocardial fibrosis [45]. The interrelationship between Gal-3 and NOX4 in the oxidative stress of PF remains to be investigated.

Another intriguing finding in this study was that we demonstrated for the first time that the expression of Gal-3 in pulmonary fibroblasts was regulated by NRF2, a classical antioxidant protein, thus uncovered another molecular mechanism linking Gal-3 with

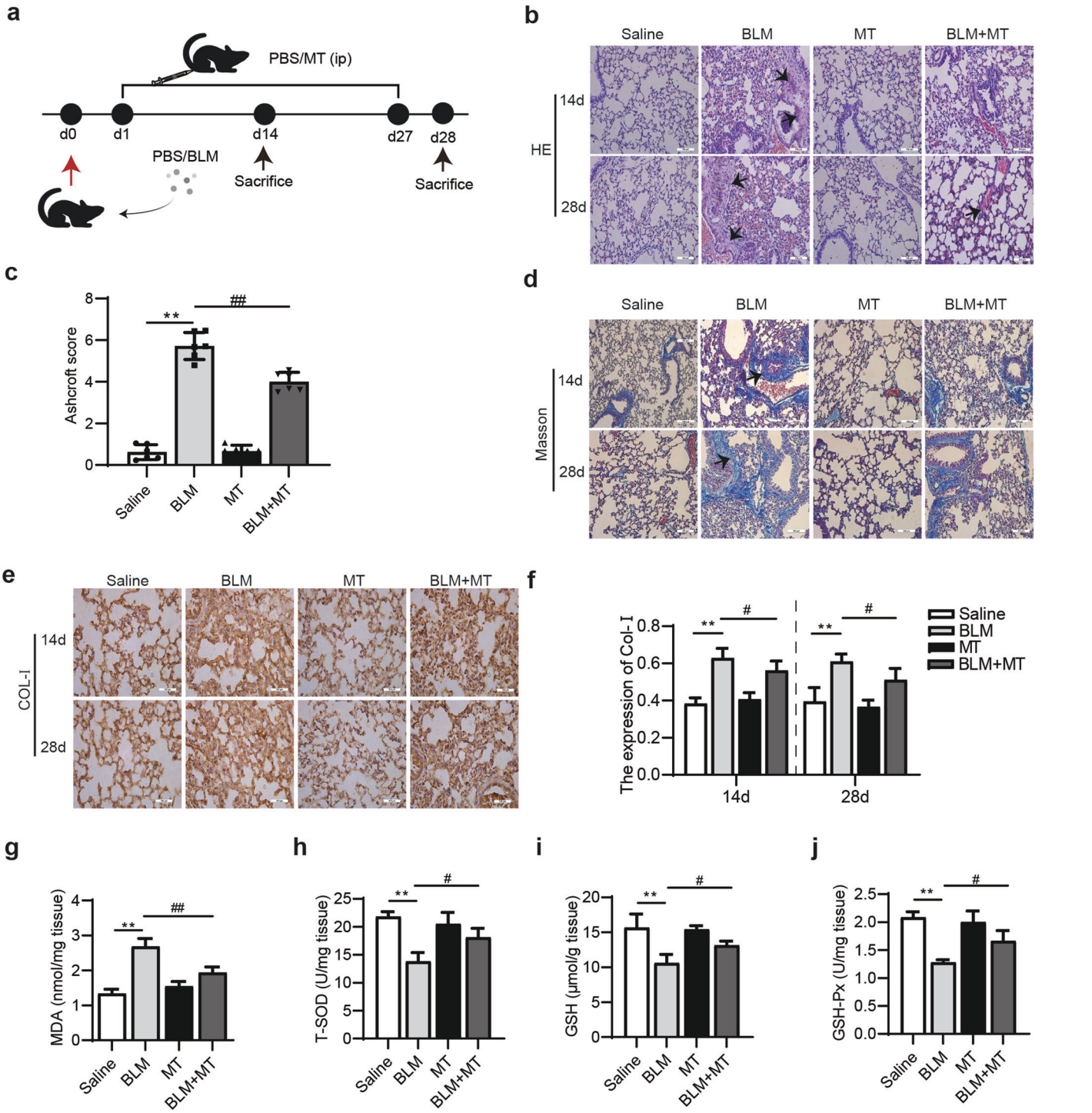

Fig. 5 MT attenuated BLM-induced PF. a Treatment schedule of BLM-induced PF mice in the presence or absence of MT. Representative histopathological sections of lung tissues by HE staining (**b**) (the typical alveolar wall thickening are marked by black arrows) and Masson's trichrome staining (**d**) (the typical collagen accumulation are indicated by black arrows), Scale bar: 100 μm. **c** Assessment of pulmonary fibrosis on the 28 day by Ashcroft score according to an eight-tier ($n = 6$). Scale bar: 100 μm. Immunohistochemical staining (**e**) and quantitation of collagen I (Col-I) (**f**) ($n = 3$). Scale bar: 100 μm. Effects of MT on oxidants and antioxidants in mouse lungs after BLM instillation and MT injection. MDA activity (**g**), T-SOD activity (**h**), GSH activity (**i**), GSH-Px activity (**j**) ($n = 3$). $^{**}P < 0.01$ versus the Saline group, $^{\#}P < 0.05$, $^{\#\#}P < 0.01$ versus the BLM group.

oxidative stress pathways. As a potential modulator of NRF2, MT mediated anti-fibrotic activities in PF by down-regulating the expression level of Gal-3. It has been reported that MT decreased circulating levels of Gal-3 in acute global cerebral ischemia in male rats, but the mechanisms were still unknown [46]. Given extensive roles of Gal-3 in various diseases, our findings provide novel important clue for understanding MT-mediated a variety of favorable biological and therapeutic activities such as antioxidant, anti-inflammatory, anti-tumor, anti-diabetic and cardio-protective effects [47], although experimental evidence remains to be supplemented.

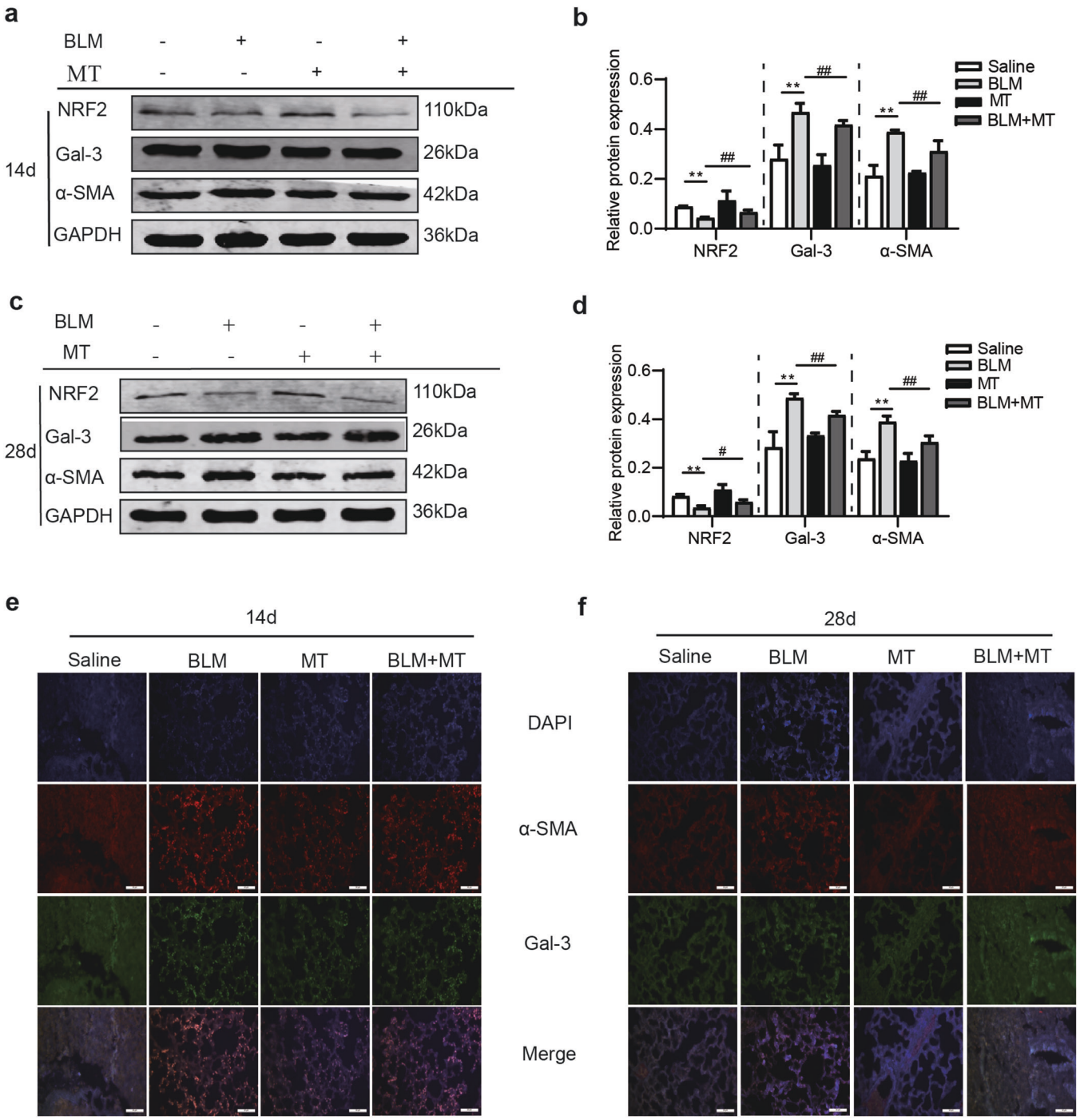

Fig. 6 MT attenuated BLM-induced PF by NRF2 upregulation and Gal-3 downregulation. Western blot results and quantitation of NRF2, Gal-3, and α-SMA levels after MT treatment. 14 d (**a**, **b**), 28 d (**c**, **d**). Relative protein levels were normalized to GAPDH ($n = 3$). **e**, **f** Immunofluorescence to detect Gal-3 (green) and α-SMA (red) expression. Scale bars: 50 μm. $^{**}P < 0.01$ versus the Saline group, $^{\#}P < 0.05$, $^{\#\#}P < 0.01$ versus the BLM group.

In summary, our data demonstrate that Gal-3 contributes to ROS production during FMD in PF, and its expression is regulated by NRF2; MT could activate NRF2 and efficiently ameliorate BLM-induced PF through suppressing Gal-3 level both in vivo and in vitro. Our study might provide a new potential therapeutic strategy for Gal-3-engaged diseases including PF.

ACKNOWLEDGEMENTS

This research was supported by the National Natural Science Foundation of China (No. 81274172, 81473267 and 81973637); the National Traditional Chinese Medicine Inheritance and Innovation "Hundreds and Thousands" Talent Project: Young Qihuang Scholar Support Project of the State Administration of Traditional Chinese Medicine in 2020.

AUTHOR CONTRIBUTIONS

YJL and JG conceived research project. YJL, HMJ, YQB, performed the experiments and data analysis. YYH, XG and CYY assisted the animal experiments. YJL, HLD, and MHC wrote the manuscript. HLD and JG supervised experiments and critically reviewed the manuscript. All authors approved the final manuscript.

ADDITIONAL INFORMATION

Competing interests: The authors declare no competing interests.

REFERENCES

1. Noble PW, Barkauskas CE, Jiang D. Pulmonary fibrosis: patterns and perpetrators. J Clin Invest. 2012;122:2756–62.
2. Guler SA, Lindell KO, Swigris J, Ryerson CJ. What is idiopathic pulmonary fibrosis? IPF Part 1. Am J Respir Crit Care Med. 2021;203:P5–P6.
3. Le Pavec J, Dauriat G, Gazengel P, Dolidon S, Hanna A, Feuillet S, et al. Lung transplantation for idiopathic pulmonary fibrosis. Presse Med. 2020;49:104026.
4. Lechowicz K, Drozdzal S, Machaj F, Rosik J, Szostak B, Zegan-Baranska M, et al. COVID-19: The potential treatment of pulmonary fibrosis associated with SARS-CoV-2 infection. J Clin Med. 2020;9:1917–36.
5. George PM, Wells AU, Jenkins RG. Pulmonary fibrosis and COVID-19: the potential role for antifibrotic therapy. Lancet Respir Med. 2020;8:807–15.
6. John AE, Joseph C, Jenkins G, Tatler AL. COVID-19 and pulmonary fibrosis: a potential role for lung epithelial cells and fibroblasts. Immunol Rev. 2021;302:228–40.
7. Mackinnon AC, Gibbons MA, Farnworth SL, Leffler H, Nilsson UJ, Delaine T, et al. Regulation of transforming growth factor-beta1-driven lung fibrosis by galectin-3. Am J Respir Crit Care Med. 2012;185:537–46.
8. Hirani N, MacKinnon AC, Nicol L, Ford P, Schambye H, Pedersen A, et al. Target inhibition of galectin-3 by inhaled TD139 in patients with idiopathic pulmonary fibrosis. Eur Respir J. 2021;57:2002559.
9. Lubrano V, Balzan S. Role of oxidative stress-related biomarkers in heart failure: galectin 3, alpha1-antitrypsin and LOX-1: new therapeutic perspective? Mol Cell Biochem. 2020;464:143–52.
10. Fulton DJR, Li X, Bordan Z, Wang Y, Mahboubi K, Rudic RD, et al. Galectin-3: a harbinger of reactive oxygen species, fibrosis, and inflammation in pulmonary arterial hypertension. Antioxid Redox Signal. 2019;31:1053–69.
11. Mendonca HR, Carpi-Santos R, da Costa Calaza K, Blanco Martinez AM. Neuroinflammation and oxidative stress act in concert to promote neurodegeneration in the diabetic retina and optic nerve: galectin-3 participation. Neural Regen Res. 2020;15:625–35.
12. Alves CM, Silva DA, Azzolini AE, Marzocchi-Machado CM, Lucisano-Valim YM, Roque-Barreira MC, et al. Galectin-3 is essential for reactive oxygen species production by peritoneal neutrophils from mice infected with a virulent strain of *Toxoplasma gondii*. Parasitology. 2013;140:210–9.
13. Yamaoka A, Kuwabara I, Frigeri LG, Liu FT. A human lectin, galectin-3 (epsilon bp/Mac-2), stimulates superoxide production by neutrophils. J Immunol. 1995;154:3479–87.
14. Liu FT, Hsu DK, Zuberi RI, Kuwabara I, Chi EY, Henderson WR Jr. Expression and function of galectin-3, a beta-galactoside-binding lectin, in human monocytes and macrophages. Am J Pathol. 1995;147:1016–28.
15. Suzuki Y, Inoue T, Yoshimaru T, Ra C. Galectin-3 but not galectin-1 induces mast cell death by oxidative stress and mitochondrial permeability transition. Biochim Biophys Acta. 2008;1783:924–34.
16. Ma Q. Role of nrf2 in oxidative stress and toxicity. Annu Rev Pharmacol Toxicol. 2013;53:401–26.
17. Zhang Z, Qu J, Zheng C, Zhang P, Zhou W, Cui W, et al. Nrf2 antioxidant pathway suppresses Numb-mediated epithelial-mesenchymal transition during pulmonary fibrosis. Cell Death Dis. 2018;9:83.
18. Qu J, Zhang Z, Zhang P, Zheng C, Zhou W, Cui W, et al. Downregulation of HMGB1 is required for the protective role of Nrf2 in EMT-mediated PF. J Cell Physiol. 2019;234:8862–72.
19. Li N, Wang Z, Gao F, Lei Y, Li Z. Melatonin ameliorates renal fibroblast-myofibroblast transdifferentiation and renal fibrosis through miR-21-5p regulation. J Cell Mol Med. 2020;24:5615–28.
20. Ding Z, Wu X, Wang Y, Ji S, Zhang W, Kang J, et al. Melatonin prevents LPS-induced epithelial-mesenchymal transition in human alveolar epithelial cells via the GSK-3beta/Nrf2 pathway. Biomed Pharmacother. 2020;132:110827.
21. Zhao X, Sun J, Su W, Shan H, Zhang B, Wang Y, et al. Melatonin protects against lung fibrosis by regulating the Hippo/YAP pathway. Int J Mol Sci. 2018;19:1118. https://doi.org/10.3390/ijms19041118.
22. Gu X, Han YY, Yang CY, Ji HM, Lan YJ, Bi YQ, et al. Activated AMPK by metformin protects against fibroblast proliferation during pulmonary fibrosis by suppressing FOXM1. Pharmacol Res. 2021;173:105844.
23. Hubner RH, Gitter W, El Mokhtari NE, Mathiak M, Both M, Bolte H, et al. Standardized quantification of pulmonary fibrosis in histological samples. Biotechniques. 2008;44:507–11.
24. Sato S, Hughes RC. Regulation of secretion and surface expression of Mac-2, a galactoside-binding protein of macrophages. J Biol Chem. 1994;269:4424–30.
25. Kasper M, Hughes RC. Immunocytochemical evidence for a modulation of galectin 3 (Mac-2), a carbohydrate binding protein, in pulmonary fibrosis. J Pathol. 1996;179:309–16.
26. Henderson NC, Mackinnon AC, Farnworth SL, Kipari T, Haslett C, Iredale JP, et al. Galectin-3 expression and secretion links macrophages to the promotion of renal fibrosis. Am J Pathol. 2008;172:288–98.
27. Duecker R, Baer P, Eickmeier O, Strecker M, Kurz J, Schaible A, et al. Oxidative stress-driven pulmonary inflammation and fibrosis in a mouse model of human ataxia-telangiectasia. Redox Biol. 2018;14:645–55.
28. Guo Z, Kozlov S, Lavin MF, Person MD, Paull TT. ATM activation by oxidative stress. Science. 2010;330:517–21.
29. Sambo P, Baroni SS, Luchetti M, Paroncini P, Dusi S, Orlandini G, et al. Oxidative stress in scleroderma: maintenance of scleroderma fibroblast phenotype by the constitutive up-regulation of reactive oxygen species generation through the NADPH oxidase complex pathway. Arthritis Rheum. 2001;44:2653–64.
30. Cho HY, Kleeberger SR. Noblesse oblige: NRF2 functions in the airways. Am J Respir Cell Mol Biol. 2014;50:844–7.
31. Cho HY, Kleeberger SR. Nrf2 protects against airway disorders. Toxicol Appl Pharmacol. 2010;244:43–56.
32. Singh A, Venkannagari S, Oh KH, Zhang YQ, Rohde JM, Liu L, et al. Small molecule inhibitor of NRF2 selectively intervenes therapeutic resistance in KEAP1-deficient NSCLC tumors. ACS Chem Biol. 2016;11:3214–25.
33. Ahmadi Z, Ashrafizadeh M. Melatonin as a potential modulator of Nrf2. Fundam Clin Pharmacol. 2020;34:11–9.
34. Leon J, Acuna-Castroviejo D, Escames G, Tan DX, Reiter RJ. Melatonin mitigates mitochondrial malfunction. J Pineal Res. 2005;38:1–9.
35. Lopez LC, Escames G, Tapias V, Utrilla P, Leon J, Acuna-Castroviejo D. Identification of an inducible nitric oxide synthase in diaphragm mitochondria from septic mice: its relation with mitochondrial dysfunction and prevention by melatonin. Int J Biochem Cell Biol. 2006;38:267–78.
36. Kleber A, Kubulus D, Rossler D, Wolf B, Volk T, Speer T, et al. Melatonin modifies cellular stress in the liver of septic mice by reducing reactive oxygen species and increasing the unfolded protein response. Exp Mol Pathol. 2014;97:565–71.
37. Henderson NC, Mackinnon AC, Farnworth SL, Poirier F, Russo FP, Iredale JP, et al. Galectin-3 regulates myofibroblast activation and hepatic fibrosis. Proc Natl Acad Sci USA. 2006;103:5060–5.
38. Ou SM, Tsai MT, Chen HY, Li FA, Tseng WC, Lee KH, et al. Identification of galectin-3 as potential biomarkers for renal fibrosis by RNA-sequencing and clinicopathologic findings of kidney biopsy. Front Med (Lausanne). 2021;8:748225.
39. Rajput VK, MacKinnon A, Mandal S, Collins P, Blanchard H, Leffler H, et al. A selective galactose-coumarin-derived galectin-3 inhibitor demonstrates involvement of galectin-3-glycan interactions in a pulmonary fibrosis model. J Med Chem. 2016;59:8141–7.
40. Jia W, Wang Z, Gao C, Wu J, Wu Q. Trajectory modeling of endothelial-to-mesenchymal transition reveals galectin-3 as a mediator in pulmonary fibrosis. Cell Death Dis. 2021;12:327.
41. Delaine T, Collins P, MacKinnon A, Sharma G, Stegmayr J, Rajput VK, et al. Galectin-3-binding glycomimetics that strongly reduce bleomycin-induced lung fibrosis and modulate intracellular glycan recognition. Chembiochem. 2016;17:1759–70.
42. Bedard K, Krause KH. The NOX family of ROS-generating NADPH oxidases: physiology and pathophysiology. Physiol Rev. 2007;87:245–313.
43. Moghadam ZM, Henneke P, Kolter J. From flies to Men: ROS and the NADPH oxidase in phagocytes. Front Cell Dev Biol. 2021;9:628991.
44. He J, Li X, Luo H, Li T, Zhao L, Qi Q, et al. Galectin-3 mediates the pulmonary arterial hypertension-induced right ventricular remodeling through interacting with NADPH oxidase 4. J Am Soc Hypertens. 2017;11:275–89
45. Sun J, Zhang L, Fang J, Yang S, Chen L. Galectin-3 mediates high-glucose-induced cardiomyocyte injury by the NADPH oxidase/reactive oxygen species pathway. Can J Physiol Pharmacol. 2020;98:826–33.
46. Fenton-Navarro B, Garduno Rios D, Torner L, Letechipia-Vallejo G, Cervantes M. Melatonin decreases circulating levels of galectin-3 and cytokines, motor activity, and anxiety following acute global cerebral ischemia in male rats. Arch Med Res. 2021;52:505–13.
47. Novais AA, Chuffa LGA, Zuccari D, Reiter RJ. Exosomes and melatonin: where their destinies intersect. Front Immunol. 2021;12:692022.